J. Fluid Mech. (2011), *vol.* 674, *pp.* 120–131.
doi:10.1017/S0022112010006439

Topological analysis of separation phenomena in liquid metal flow in sudden expansions. Part 1. Hydrodynamic flow

C. MISTRANGELO†

Karlsruhe Institute of Technology (KIT), IKET, Herrmann-von-Helmholtz-Platz 1, Eggenstein-Leopoldshafen 76344, Germany

(Received 1 February 2010; revised 11 October 2010; accepted 15 December 2010; first published online 23 March 2011)

Numerical simulations are performed to study three-dimensional hydrodynamic flows in a sudden expansion of rectangular ducts. Separation phenomena are investigated through the analysis of flow topology and streamline patterns. Scaling laws describing the evolution of the reattachment length of the vortical areas that appear behind the cross-section enlargement are derived. The results discussed in this paper are required as a starting point to investigate the effects of an applied homogeneous magnetic field on separation phenomena in a geometry with a sudden expansion.

Key words: channel flow, separated flow, topological fluid dynamics

1. Introduction

In the past, flows in expanding geometries have attracted considerable attention because, although the geometric configuration is simple, the resulting flow field behind the cross-section enlargement has complex features including separation and reattachment regions. Their study is of great practical interest since the existence of recirculations has an influence on heat, mass and momentum transport and therefore on the performance of engineering systems. The present work has been carried out with the aim of obtaining a good understanding of the hydrodynamic flow in a specific sudden expansion. In this paper, only the main flow features are presented, whose discussion is required as a starting point for the analysis of the influence of magnetic fields on flow separation (Mistrangelo 2011).

In a duct with a sudden cross-section enlargement, a pressure increase occurs behind the expansion. If the flow close to the wall, in the boundary layer, is sufficiently slowed down by surface friction and adverse pressure gradient, the motion of the near-wall fluid is eventually brought to rest at the so-called *separation point* or line. At this location the streamline closest to the surface leaves the wall and the boundary layer separates (Maskell 1955). This phenomenon is associated with the formation of reversed flow and vortices. Separation of a steady, two-dimensional boundary layer was explained first by Prandtl (1904), who defined a criterion stating that at separation and reattachment points the wall shear stress ($\tau_w = \rho\nu\,\partial u/\partial y$, where u is the axial velocity parallel to the wall and y is the wall-normal coordinate) is zero. However, for three-dimensional (3D) or unsteady separated flows, the point of vanishing wall

† Present address: KIT, Campus North, Postfach 3640, 76021 Karlsruhe, Germany. Email address for correspondence: chiara.mistrangelo@kit.edu

shear does not necessarily coincide with separation (Williams 1977). Lighthill (1963) suggested the use of the *theory of critical points* introduced by Legendre (1956) for describing the separation of 3D boundary layers. Critical points are singularities in the flow field where the velocity becomes zero and the direction of the vector quantity under consideration (the streamline slope) is undetermined. These singular points can be classified into *nodes* and *saddle points* (Hunt *et al.* 1978). The former ones include nodal points and foci. It can be observed that a three-dimensional flow tends to separate along a line and the shear stress at the wall is equal to zero at a finite number of points along it. The number and type of these singular points must satisfy certain topological rules (Lighthill 1963; Hunt *et al.* 1978).

The three-dimensional features of the flow can be deduced and interpreted by studying limiting streamline patterns and analysing the flow topology, namely distribution, type and relations of critical points (Tobak & Peake 1982; Délery 2001). *Limiting streamlines* are so called because they are drawn on a plane whose distance from a no-slip wall tends to zero (Maskell 1955). In a separation process, limiting streamlines converge towards a common line called *separation line*. Instead, a *reattachment line* is characterized by the fact that the streamlines diverge from it. Therefore, Prandtl's separation criterion based on the identification of isolated wall-shear zeros valid for 2D flows is replaced for 3D flows by a criterion of convergence and divergence of skin-friction lines to and from a critical line. Mathematical rules for locating flow separation in three-dimensional flows have been derived by Surana, Grunberg & Haller (2006) by applying the nonlinear dynamics system theory as used by Haller (2004) for two-dimensional flows.

Two-dimensional incompressible laminar flows in symmetric sudden expansions have been the subject of several numerical and experimental investigations. According to experimental studies (Durst, Mellin & Whitelaw 1974; Cherdron, Durst & Whitelaw 1978; Sobey & Drazin 1986; Fearn, Mullin & Cliffe 1990; Durst, Pereira & Tropea 1993) at sufficiently low Reynolds numbers Re, a unique steady state solution is found. The resulting flow field is symmetric with respect to the channel middle plane, with two recirculation zones of equal size near the corners of the expansion. Their length increases linearly with Re. At a critical value of the Reynolds number, which depends on the expansion ratio of the duct, the steady symmetric solution becomes unstable, bifurcates at a pitchfork point from where a pair of stable, asymmetric solutions emerges (Fearn *et al.* 1990). This behaviour is called exchange of stability and the bifurcation is classified as supercritical. Experimental findings have been confirmed by numerical investigations (Durst *et al.* 1993; Alleborn *et al.* 1997; Drikakis 1997). With increasing the Reynolds number, the asymmetry becomes stronger and then a third separation region appears downstream of the smaller recirculation zone (Durst *et al.* 1993). As the Reynolds number is further increased, the flow becomes time-dependent and the unsteadiness is associated with three-dimensional effects (Fearn *et al.* 1990; Durst *et al.* 1993). For larger Re, the flow finally becomes turbulent.

In contrast to the significant number of 2D investigations, only few studies of 3D flows in sudden expansions have been performed (Baloch, Townsend & Webster 1995; Chiang, Sheu & Wang 2000; Schreck & Schäfer 2000; Chiang *et al.* 2001). Williams & Baker (1997) carried out three-dimensional numerical simulations of hydrodynamic flow over a backward-facing step of high aspect ratio. They found that, depending on the Reynolds number, the flow in the separation region becomes highly three-dimensional due to the effect of the sidewalls. The presence of the sidewalls results in the formation of a spiralling motion from the lateral wall of the channel to the middle plane. The occurrence of this vortical structure was supported by the

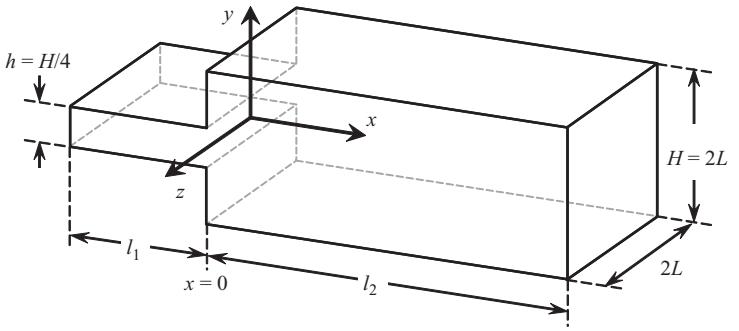

FIGURE 1. Sketch of the geometry used for the numerical study. The expansion ratio is $H/h = 4$. The geometry expands along the y-direction and the cross-section enlargement is located at $x = 0$. The quantity L is chosen as characteristic size of the channel.

numerical results of Chiang & Sheu (1999) and by experiments and simulations of Tylli, Kaiktsis & Ineichen (2002). Chiang *et al.* (2000) studied the effects of the sidewalls on flow structures in a sudden expansion and showed that, for a fixed expansion ratio, a critical aspect ratio exists beyond which an initially symmetric flow becomes asymmetric.

2. Problem formulation

The three-dimensional flow of a viscous, incompressible fluid is studied in a rectangular channel of width $2L$ and height h, which expands symmetrically, with right angles, into a duct having same width and high $H = 4h = 2L$ as shown in figure 1. The geometry is chosen according to the features of the experimental test section used in the MEKKA laboratory of the Karlsruhe Institute of Technology (Bühler & Horanyi 2006). The flow field is described in a Cartesian coordinate system such that x, y and z are the streamwise, the vertical and the spanwise directions, $y = z = 0$ is the axis of the channel and the junction between small and large duct is at $x = 0$. The inlet of the channel is far enough upstream not to influence the flow pattern near the sudden expansion and the duct is sufficiently long to ensure fully developed conditions at the exit.

For the following analysis, all the dimensions are scaled by half of the channel width, $L = 47$ mm, so that the non-dimensional size of the inlet duct is $-0.25 \leqslant y \leqslant 0.25$ and $-1 \leqslant z \leqslant 1$, and that of the outlet channel is $-1 \leqslant y \leqslant 1$. The velocities are normalized by the average value v_0 in the exit channel so that the mean dimensionless velocity in the large duct becomes $\bar{v}_2 = 1$ and that in the small duct becomes $\bar{v}_1 = 4$.

The three-dimensional, incompressible flow in the ducts is governed by the dimensionless equations accounting for conservation of momentum and mass:

$$\frac{\partial \boldsymbol{v}}{\partial t} + (\boldsymbol{v} \cdot \nabla)\, \boldsymbol{v} = -\nabla p + \frac{1}{Re}\nabla^2 \boldsymbol{v}, \quad \nabla \cdot \boldsymbol{v} = \boldsymbol{0}. \tag{2.1}$$

The variables $\boldsymbol{v}$ and p denote velocity and pressure scaled by the reference quantities v_0 and ρv_0^2, respectively. The non-dimensional group governing the problem is the Reynolds number $Re = v_0 L/\nu$, which represents the importance of inertia compared with viscous forces. The fluid density ρ and the kinematic viscosity ν are assumed to be constant.

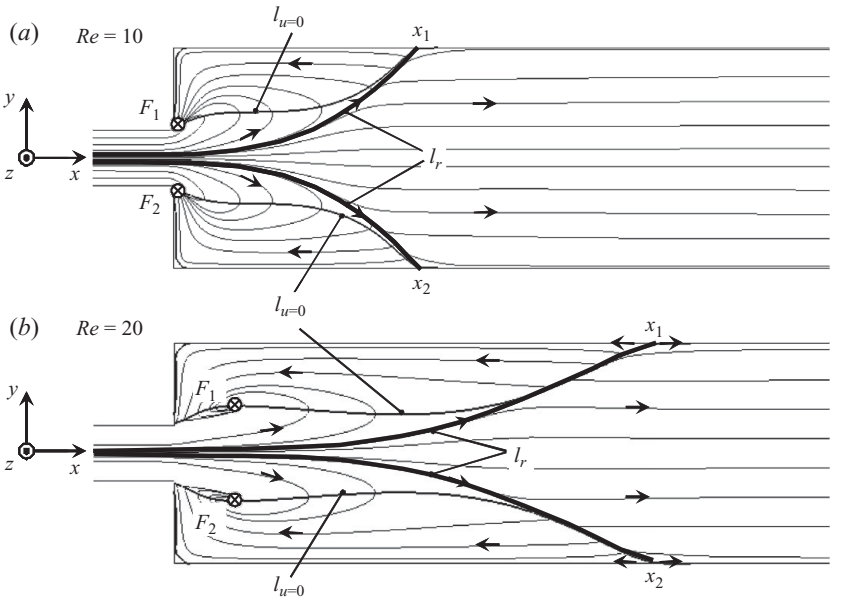

FIGURE 2. Limiting streamlines on the lateral wall of the duct for the symmetric flows at (*a*) $Re = 10$ and (*b*) $Re = 20$. Lines $l_{u=0}$ indicate locations where the u-velocity component is zero or changes sign. The points where the reattachment lines l_r meet the top and bottom walls of the duct are marked by x_1 and x_2, respectively. The foci, centre of the vortical motion, are called F_1 and F_2.

3. Results and discussion

The numerical analysis has been carried out by using an extended version of the finite volume CFD code CFX-5.6, where the pressure–velocity coupling is based on the SIMPLE (semi-implicit method for pressure-linked equations) algorithm and an algebraic multi-grid method is used to obtain the solution (for more details, see Mistrangelo 2011). A biased mesh is used in all the directions with nodes clustered at the walls and across the sudden expansion. Upstream and downstream where the flow approaches fully developed conditions the number of nodes per unit length is reduced. The length of the square outlet duct as well as the total number of points has been changed depending on the set of parameters under study. Grid sensitivity studies have been performed to obtain mesh-independent results.

In the following, the outlined concepts of the theory of critical points and limiting streamline patterns are employed to describe the three-dimensional separated flow occurring behind a symmetric sudden expansion. In order to achieve a good understanding of the flow features, a topological study of the velocity field is performed. The location of critical points in the pattern of skin-friction lines is found as the position where both components of the wall shear stress on the plane of interest change sign or vanish simultaneously.

The numerical analysis shows that at low Reynolds number, the flow is symmetric with respect to the plane $y = 0$ and the size of the recirculations increases with the Reynolds number. In figure 2, limiting streamlines are plotted on the lateral wall of the channel for the symmetric flows at $Re = 10$ and $Re = 20$. The lines $l_{u=0}$ indicate the points on the considered wall where the axial velocity component changes its sign or becomes zero. They pass through the critical points of the velocity field and give an indication of the reattachment length of the separation region.

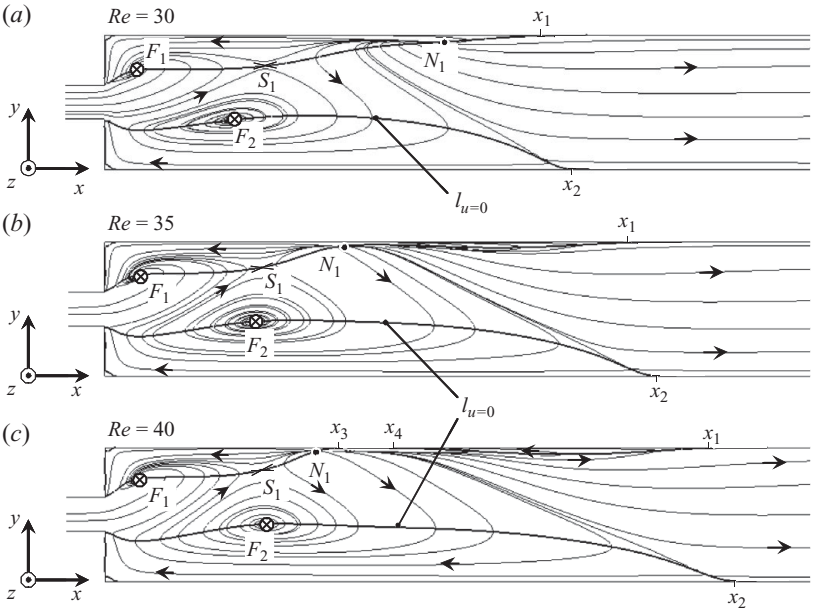

FIGURE 3. Limiting streamlines on the lateral wall of the channel for asymmetric flows at (*a*) $Re = 30$, (*b*) $Re = 35$ and (*c*) $Re = 40$. The saddle point and the node that appear for $Re > Re_{c1} \simeq 27$ are labelled S_1 and N_1, respectively.

The flow topology on the lateral wall consists of two half saddle points or stagnation points, x_1 and x_2, which correspond to the reattachment locations of the primary recirculation zone on the upper and lower walls of the channel, and by two stable foci (F_1 and F_2), which the streamlines spiral on. The identified foci are the traces on the lateral wall of a 3D spiralling path that transports the fluid from the sidewalls to the middle plane of the duct at $z = 0$. Each focus is the starting point of an isolated line, which the other streamlines in the separation region spiral around taking on helical shape. Henceforth, this line will be referred to as *vortex core line*.

It has been observed that the flow coming from points very close to the lateral walls enters the large duct and starts swirling around the vortex core line reaching the middle plane of the channel. Fluid injected farther from the sidewalls turns only a few times around the vortex core line and it only approaches the symmetry plane at $z = 0$ without touching it. Particles released at a sufficiently large distance from the lateral walls move directly downstream and they are no longer trapped into the vortices.

In figure 2, a reattachment line l_r can be identified as the one from which the limiting streamlines diverge. It meets top and bottom walls of the duct at the stagnation points x_1 and x_2. This line is the trace on the lateral wall of a surface that separates the reversed flow from the rest of the stream that moves directly towards the exit of the duct. With increasing the Reynolds number, the recirculations become longer and the two foci move further downstream as shown in figure 2(*b*).

Beyond a critical value of the Reynolds number, $Re_{c1} \cong 27$, the flow becomes asymmetric and as a result the topology on the sidewall changes, as shown in figure 3(*a*) for the flow at $Re = 30$. At these flow conditions, two foci (F_1 and F_2) and two reattachment points (x_1 and x_2) are present on the lateral wall like for

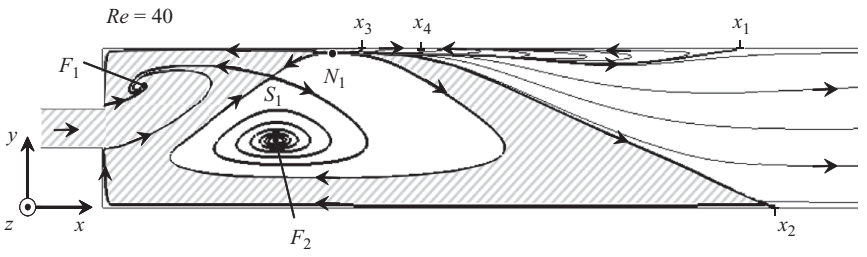

FIGURE 4. Characteristic streamlines originating from node N_1 drawn on the lateral wall of the channel for the flow at $Re = 40$. The streamlines in the dashed areas enter focus F_1, those in the central white zone feed the vortex with centre F_2.

the symmetric flow. However, two additional critical points appear which describe the interaction between primary vortices. They consist of a node N_1 that feeds the recirculations and a saddle point S_1 that separates the two bubbles. At a saddle point only two lines, called separatrices, pass through the critical point whereas the other streamlines avoid it and take on hyperbolic shape moving asymptotically along the two characteristic lines.

In this new topological configuration, the reattachment lengths x_1 and x_2 of the primary separation zones remain comparable by increasing the Reynolds number and the longitudinal distance between the node N_1 and the stagnation point x_1 becomes larger. This is due to the fact that by rising the Reynolds number the two singularities, N_1 and x_1, move in opposite direction as shown in figure 3(b) for the flow at $Re = 35$. Downstream immediately after node N_1, next to the top wall of the duct, the fluid strongly slows down and at $Re = Re_{c2} \cong 37$ the limiting streamline closest to the upper wall touches it in a point near node N_1 and a secondary recirculation appears. Two new characteristic points named x_3 and x_4 are present, as illustrated in figure 3(c) for the flow at $Re = 40$. The first point is now the reattachment point of the smaller bubble of the primary recirculation and x_4 marks the position where the secondary separation zone forms. The velocity between x_3 and x_4 is very small and this is one of the reasons that make it difficult to identify exactly the occurrence and position of these two points.

In figure 4, characteristic limiting streamlines originating from node N_1 are depicted on the lateral wall of the duct for the flow at $Re = 40$. Streamlines that flow into the dashed areas enter focus F_1 and feed the smaller primary recirculation, while those in the central white zone form the larger bubble with centre F_2. It is interesting to note that the backflow that occurs after x_4 remains localized near the corners of the duct and it transports the fluid downstream, while the primary vortices have a preferential direction from the lateral walls to the middle plane of the channel. This could be the reason why at the sidewall no focus can be identified for the additional reversed flow zone.

Differences are observed between the development of the separation regions on the sidewalls ($z = \pm 1$) and the middle plane ($z = 0$) of the duct: the described points N_1 and S_1 as well as the secondary recirculation disappear at some distance from the lateral walls where the flow pattern resembles that of the 2D hydrodynamic flow. This can be seen in figure 5, where limiting streamlines are drawn on the duct symmetry plane at $z = 0$ for flows at $Re = 20$, 30, 35 and 40. The reattachment points on the top and bottom of the channel are named x_{01} and x_{02}, respectively, and the foci are called F_{s1} and F_{s2}. The latter ones are unstable and the velocity streamlines first move

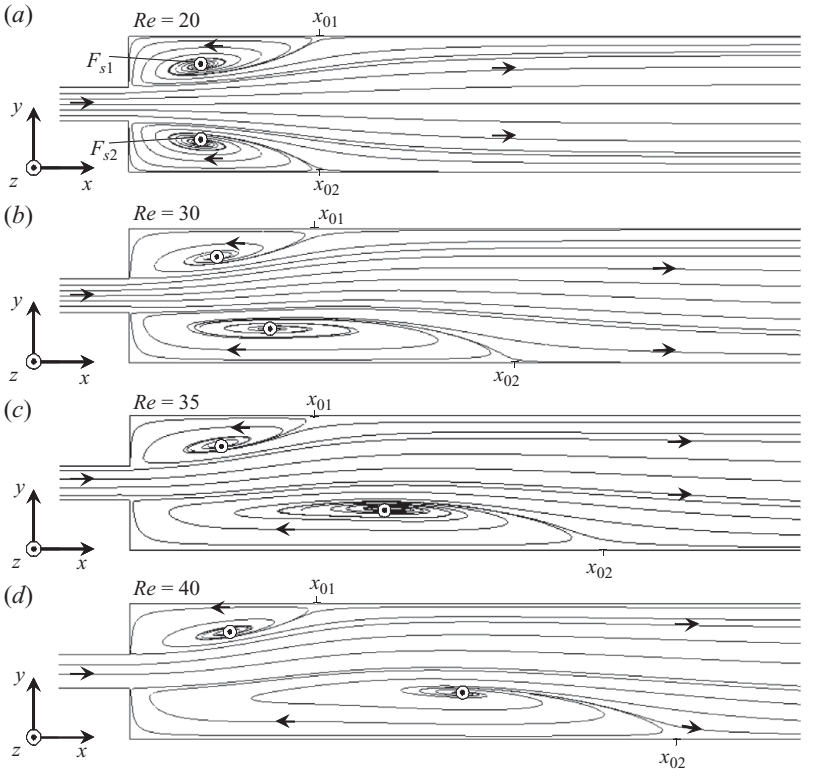

FIGURE 5. Limiting streamlines on the symmetry plane of the duct at $z=0$ for the flow at (a) $Re=20$, (b) $Re=30$, (c) $Re=35$ and (d) $Re=40$. The reattachment points at the top and bottom of the channel are named x_{01} and x_{02}, respectively. The foci are called F_{s1} and F_{s2}.

towards them, flowing around a vortex core line, and then spiral out. On the contrary, foci F_1 and F_2 on the lateral walls are stable (attracting). The different behaviour can be seen in figure 6, where a vortical flow path is visualized as an example for the symmetric flow at $Re=20$. The discussed critical points and characteristic lines $l_{u=0}$ and l_r are also shown.

The evolution of reattachment (x_1, x_2 and x_3) and separation (x_4) points on the lateral wall of the channel as a function of the Reynolds number is illustrated in figure 7(a). Even when the flow becomes asymmetric ($Re > Re_{c1}$), the axial position of x_1 and x_2 on the lateral wall is comparable. Scanning the axial location of the node N_1, typical of asymmetric flows (see figures 3 and 4), in the range $Re_{c1} < Re < Re_{c2}$, it is found that its position changes following the dotted curve drawn in figure 7(a). If we consider the diagram formed by x_2, N_1 and x_3, a pitchfork-like bifurcation similar to that for the points on the middle plane (figure 7b) is obtained. This diagram describes the changes in the size of the bubbles forming the primary recirculations.

With increasing Reynolds number, the additional separation zone included between x_4 and x_1 moves downstream as suggested by the raising of the distance between the reattachment point x_3 of the small recirculation and the separation point x_4 of the secondary flow.

Regarding the evolution of the recirculation lengths on the symmetry plane $z=0$, shown in figure 7(b), it can be noted that after the onset of the asymmetry, by increasing the supercritical Reynolds number ($Re > Re_{c1}$), one of the recirculations

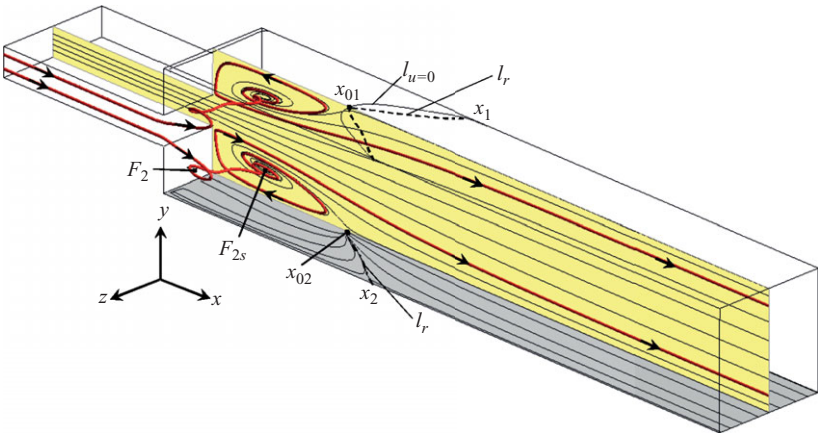

FIGURE 6. Limiting streamlines on the bottom of the duct and solution trajectories on the middle plane ($z=0$) for the symmetric flow at $Re=20$. The reattachment lines l_r on top and bottom of the channel meet the lateral walls at x_1 and x_2, and the symmetry plane at x_{01} and x_{02}. Here F_2 is a stable focus (attracting) and F_{2s} is an unstable one (repelling).

becomes smaller, x_{01}, and finally remains almost constant, whereas the other one, x_{02}, grows progressively with the Reynolds number. The backflow region is shorter than that on the lateral wall. The bifurcation diagram for the flow on the symmetry plane is analogous to that for the 2D hydrodynamic flow. The latter has also been numerically investigated and the identified critical Reynolds number corresponding to the symmetry-breaking bifurcation point ($Re_{c2D} \cong 18$) agrees well with the results in the literature (Drikakis 1997; Revuelta 2005). The comparison with the solution for the 3D flow confirms the stabilizing effect of the sidewall, as observed by Cherdron *et al.* (1978) and Schreck & Schäfer (2000), which results in a higher critical Reynolds number for the onset of asymmetry for the three-dimensional flow ($Re_{c3D} \cong 27$).

It is also worth describing the changes of the flow topology near the bottom wall of the channel when raising the Reynolds number. In figure 8, the limiting streamlines are depicted on the lower wall of the duct for the symmetric flows at $Re=10$ and $Re=25$. At $Re=10$, a node N_+ acting as a streamline source is present on the reattachment line l_r and a sink N_- lies on the separation line l_s close to the expansion wall. This line indicates the presence at the duct corners of small vortical paths. For higher Reynolds numbers (e.g. $Re=25$ in figure 8*b*) two sinks N_- appear near the external corners of the expansion wall, on the separation line, and they are associated with a saddle point S_2 located at $z=0$. The topology along the reattachment line is equal to that described for smaller Reynolds numbers.

Above the symmetry-breaking Reynolds number, Re_{c1}, the topological structure on the bottom of the duct changes as depicted in figure 9, where limiting streamlines are drawn for the asymmetric flow at $Re=30$. The node N_+ that was present on the reattachment line, at $z=0$, splits into two nodes of reattachment and a new saddle point S_1 appears between them. With increasing further the Reynolds number, these two nodes move towards the lateral walls. The separation line that connects the two saddle points S_1 and S_2 prevents the limiting streamlines that emerge from nodes N_+ from crossing the centreline at $z=0$.

The flow topology becomes more complex for larger Reynolds numbers even in the laminar stationary regime. This is indicated by an increasing number of critical points which describe the kinematic aspects of the streamlines.

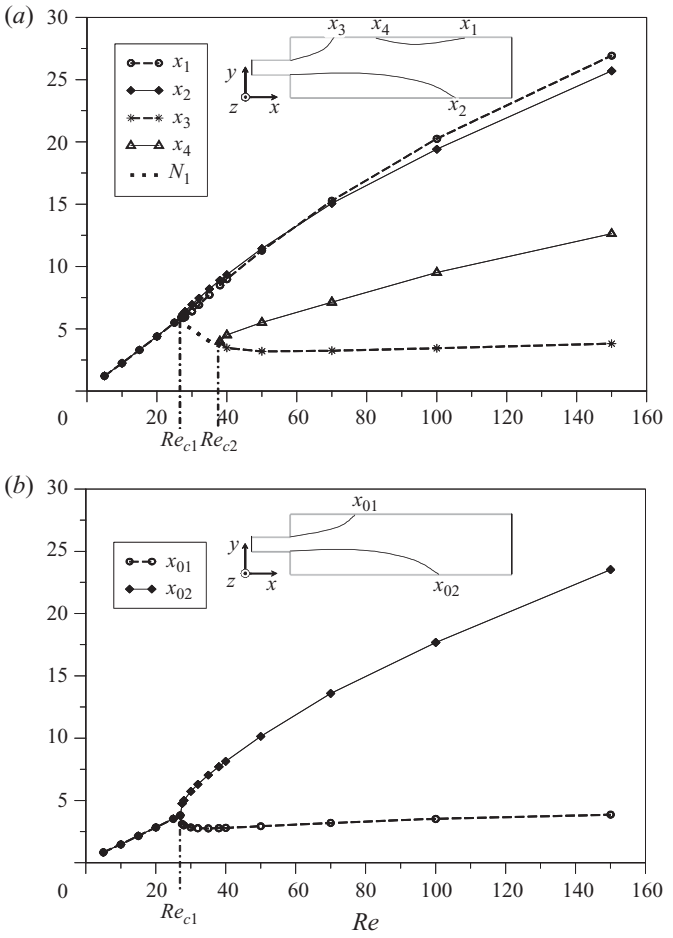

FIGURE 7. Locations of reattachment (x_1, x_2, x_3) and separation (x_4) points of the recirculations (a) on the lateral wall of the duct and (b) on the symmetry plane at $z=0$ as a function of the Reynolds number. In (a), the dotted line drawn between Re_{c1} and Re_{c2} indicates the axial position of node N_1 (see figures 3 and 4).

4. Conclusions

Hydrodynamic flows in a sudden expansion of rectangular ducts with expansion ratio equal 4 have been studied numerically with the aim of achieving a good insight into the separation phenomena that occur in this geometry.

The flow features have been analysed by performing a topological study of the velocity field in the duct, i.e. by identifying critical points and characteristic curves connecting them. Limiting streamline patterns have been used for this purpose. Changes in the type and number of these topological elements allow inferring to a certain extent the structure of the entire velocity field and the interaction between the various separation and vortical zones. It has been found that the increase of complexity of the flow field with the Reynolds number is well described by the occurrence of a larger number of critical points.

The numerical analysis shows that for $Re < Re_{c1} \simeq 27$, two recirculations of the same size are present in the channel and their reattachment length increases linearly with the Reynolds number. For larger Reynolds numbers, the flow is asymmetric:

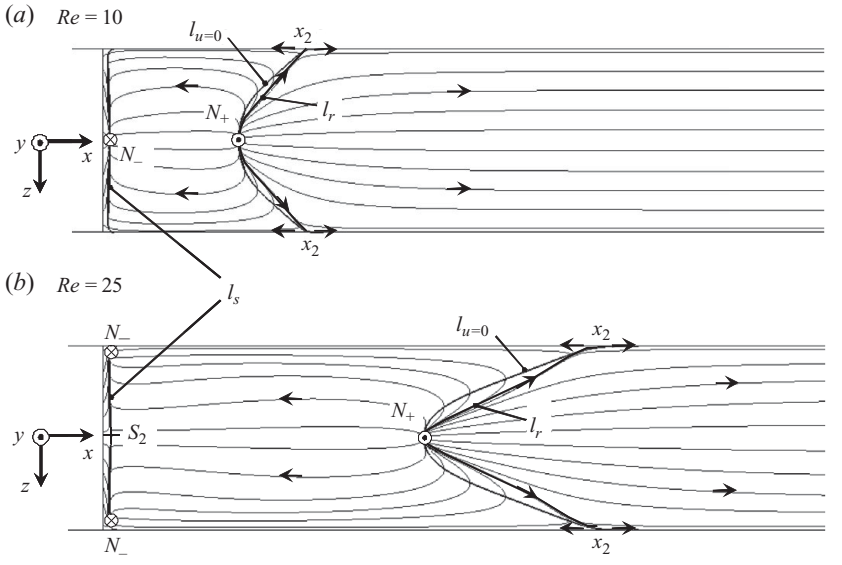

FIGURE 8. Limiting streamlines on the bottom of the channel for the symmetric flows at (*a*) $Re = 10$ and (*b*) $Re = 25$. By increasing the Reynolds number, the topology close to the reattachment line l_r remains the same, while it changes near the expansion wall along the separation line l_s (new saddle point S_2).

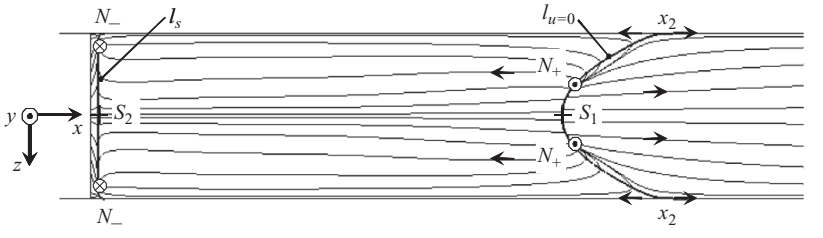

FIGURE 9. Limiting streamlines on the bottom of the duct for the asymmetric flow at $Re = 30$. Downstream along the reattachment line new topological features are present: two reattachment nodes N_+ acting as sources of streamlines and a saddle point S_1.

one bubble shrinks and the other one becomes longer. It should be noted that it is equally probable to get a solution that is mirrored with respect to the plane $y = 0$ compared with that described in the paper. For $Re > Re_{c2} \simeq 37$, a secondary recirculation appears downstream, behind the smaller primary vortical zone.

For all the investigated Reynolds numbers ($Re \leqslant 150$), the topology of the flow on the symmetry plane at $z = 0$ resembles that of the 2D flow. The additional critical points present on the lateral walls when the flow is asymmetric as well as the secondary vortex disappear at some distance from the wall. The evolution of the separation areas, in terms of reattachment and separation points, is represented by a pitchfork-like bifurcation diagram analogous to that obtained for the two-dimensional flow in the same geometry. However, the critical symmetry-breaking Reynolds number is larger for the 3D flows ($Re_{c3D} \cong 27 > Re_{c2D} \cong 18$), indicating a stabilizing effect of the sidewalls on the velocity field.

As already mentioned, the present paper is intended as a brief overview of the main topological characteristics of hydrodynamic flows in a specific sudden expansion.

An exhaustive description of this fundamental hydrodynamic problem is out of the scope of this paper. The results shown here are a starting point required to assess the effects of an imposed uniform magnetic field on separation phenomena in the considered geometry as discussed in Part 2 (Mistrangelo 2011). Only the knowledge of the complexity of the hydrodynamic flow allows appreciating the strong action of the electromagnetic forces on flow structures and their role in the balance of forces established in the ducts.

REFERENCES

Alleborn, N., Nandakumar, K., Raszillier, H. & Durst, F. 1997 Further contributions on the two-dimensional flow in a sudden expansion. *J. Fluid Mech.* **330**, 169–188.

Baloch, A., Townsend, P. & Webster, M. F. 1995 On two- and three-dimensional expansion flows. *Comput. Fluids* **24** (8), 863–882.

Bühler, L. & Horanyi, S. 2006 Experimental investigations of MHD flows in a sudden expansion. *Tech. Rep.* FZKA 7245. Forschungszentrum Karlsruhe.

Cherdron, W., Durst, F. & Whitelaw, J. H. 1978 Asymmetric flows and instabilities in symmetric ducts with sudden expansions. *J. Fluid Mech.* **84** (1), 13–31.

Chiang, T. P. & Sheu, T. W. H. 1999 A numerical revisit of backward-facing step flow problem. *Phys. Fluids* **11** (4), 862–874.

Chiang, T. P., Sheu, T. W. H., Hwang, R. R. & Sau, A. 2001 Spanwise bifurcation in plane-symmetric sudden-expansion flows. *Phys. Rev.* E **65**, 016306 (1–16).

Chiang, T. P., Sheu, T. W. H. & Wang, S. K. 2000 Side wall effects on the structure of laminar flow over a plane-symmetric sudden expansion. *Comput. Fluids* **29** (5), 467–492.

Délery, J. M. 2001 Robert Legendre and Henri Werlé: Towards the elucidation of three-dimensional separation. *Annu. Rev. Fluid Mech.* **33**, 129–154.

Drikakis, D. 1997 Bifurcation phenomena in incompressible sudden expansion flows. *Phys. Fluids* **9** (1), 76–87.

Durst, F., Mellin, A. & Whitelaw, J. H. 1974 Low Reynolds number flow over a plane symmetric sudden expansion. *J. Fluid Mech.* **64** (1), 111–128.

Durst, F., Pereira, J. C. F. & Tropea, C. 1993 The plane symmetric sudden-expansion flow at low Reynolds numbers. *J. Fluid Mech.* **248**, 567–581.

Fearn, R. M., Mullin, T. & Cliffe, K. A. 1990 Nonlinear flow phenomena in a symmetric sudden expansion. *J. Fluid Mech.* **211**, 595–608.

Haller, G. 2004 Exact theory of unsteady separation for two-dimensional flows. *J. Fluid Mech.* **512**, 257–311.

Hunt, J. C. R., Abell, C. J., Peterka, J. A. & Woo, H. 1978 Kinematical studies of the flows around free or surface-mounted obstacles: applying topology to flow visualization. *J. Fluid Mech.* **86**, 179–200.

Legendre, R. 1956 Séparation de l'écoulement laminaire tridimensionnel. *La Recherche Aéronautique* **54**, 3–8.

Lighthill, M. J. 1963 Attachment and separation in three-dimensional flows. In *Laminar Boundary Layers* (ed. L. Rosenhead), chap. 2, 2.6, pp. 72–82. Oxford University Press.

Maskell, E. C. 1955 Flow separation in three dimensions. *Tech. Rep.* 2565. Royal Aircraft Establishment, Farnborough, England.

Mistrangelo, C. 2011 Topological analysis of separation phenomena in liquid metal flow in sudden expansions. Part 2. Magnetohydrodynamic flow. *J. Fluid Mech.* doi:10.1017/S0022112011000607.

Prandtl, L. 1904 Über Flüssigkeitsbewegung bei sehr kleiner Reibung. In *Proceedings of the Third International Mathematics Congress, Heidelberg, Germany*, pp. 484–491.

Revuelta, A. 2005 On the two-dimensional flow in a sudden expansion with large expansion ratios. *Phys. Fluids* **17**, 028102.

Schreck, E. & Schäfer, M. 2000 Numerical study of bifurcation in three-dimensional sudden channel expansions. *Comput. Fluids* **29** (5), 583–593.

Sobey, I. J. & Drazin, P. G. 1986 Bifurcations of two-dimensional channel flows. *J. Fluid Mech.* **171**, 263–287.

Surana, A., Grunberg, O. & Haller, G. 2006 Exact theory of three-dimensional flow separation. Part 1. Steady separation. *J. Fluid Mech.* **564**, 57–103.

Tobak, M. & Peake, D. J. 1982 Topology of three-dimensional separated flows. *Annu. Rev. Fluid Mech.* **14**, 61–85.

Tylli, N., Kaiktsis, L. & Ineichen, B. 2002 Sidewall effects in flow over a backward-facing step: experiments and numerical simulations. *Phys. Fluids* **14** (11), 3835–3845.

Williams, J. C. 1977 Incompressible boundary-layer separation. *Annu. Rev. Fluid Mech.* **9**, 113–144.

Williams, P. T. & Baker, A. J. 1997 Numerical simulations of laminar flow over a 3D backward-facing step. *Intl J. Numer. Meth. Fluids* **24**, 1159–1183.